J Nanopart Res (2018) 20: 29
https://doi.org/10.1007/s11051-017-4118-x

RESEARCH PAPER

Synergetic scattering of SiO_2 and Ag nanoparticles for light-trapping enhancement in organic bulk heterojunction

Huan Yang · Qiuyu Ding · Ben Q. Li · Xinbing Jiang · Manman Zhang

Received: 23 October 2017 / Accepted: 22 December 2017 / Published online: 1 February 2018

Abstract Though noble metal nanoparticles have been explored to enhance the performance of the organic solar cell, effect of dielectric nanoparticles, and coupled effect of dielectric and metal nanoparticles, have rarely been reported, if at all, on organic solar cell. This work reports an experimental study on synergetic scattering of SiO_2 and Ag nanoparticles in a bulk organic heterojunction for the broadband light absorption enhancement. The wavelength scale SiO_2 particles were arranged as a monolayer on the surface of the solar cell to guide incident light into the active layer and prolong the effective optical length of the entered energy. This is achieved by the excitation of whispering gallery modes in SiO_2 nanoparticles and by leaky mode radiation. When small size Ag particles were incorporated into the transport layer of the solar cell, synergetic scattering of SiO_2 and Ag nanoparticles is formed by coupling of the whispering gallery mode of closely arranged SiO_2 particles atop and collaborative localized surface plasma resonance scattering of Ag nanoparticles dispersed in the transport layer. As a result, the performance of the organic solar cell is greatly enhanced and the short-circuit current density has an improvement of 42.47%. Therefore, the organic solar cell incorporated with SiO_2 and Ag particles presents a meaningful strategy to achieve high energy-harvesting performance.

Keywords Nanoparticles · Coupled scattering · Heterojunction solar cell · P3HT · Nanocomposites · Energy conversion

H. Yang · Q. Ding · B. Q. Li (✉) · X. Jiang · M. Zhang
Micro- and Nano-Manufacturing Research Center, State Key Laboratory for Manufacturing Systems Engineering, Xi'an Jiaotong University, Xi'an, Shaanxi 710049, China
e-mail: benqli@umich.edu

B. Q. Li
Department of Mechanical Engineering, College of Engineering and Computer Science, University of Michigan-Dearborn, Dearborn, MI 48128, USA

Introduction

Organic semiconductor heterojunction has been studied for years for solar energy-harvesting applications. The continuous effort in this area is derived from the potential advantages of organic solar cells such as low cost, light weight, mechanical flexibility, and ease to manufacture (Krebs et al. 2004; Li et al. 2012; Luo et al. 2016; Yu et al. 1995). In general, the performance of solar cells is determined by two key processes: (i) light trapping and exciton generation and (ii) exciton dissociation, charge carrier transport, and collection. Much of the current effort has been on optimizing the morphology of the active photovoltaic layer and the charge transport properties of the absorber (Dang et al. 2011; Lee et al. 2008; Li et al. 2007; Ma et al. 2005). Because of the low charge carrier mobility and short exciton diffusion length, the thickness of organic photoactive layer is still limited to within a few hundred nanometers, leading to a low light absorption in the organic heterojunction. Therefore, measures are needed to enhance the light absorption while maintaining efficient exciton dissociation, charge carrier transport, and

collection. Thus far, various light-trapping techniques have been proposed to improve the photon-harvesting efficiency, including the application of diffraction gratings (Na et al. 2007; Niggemann et al. 2004), periodic nanostructures (Chou and Chen 2014; Mariani et al. 2010; Nalwa et al. 2011; Yang and Forrest 2008), and nanoparticles (Cao et al. 2014; Gan et al. 2013; Gollu et al. 2015; Jang et al. 2016; Kalfagiannis et al. 2012; Liu et al. 2014; Shahin et al. 2012; Shao et al. 2017). In general, fabrication of nanostructured layers often involves rather complicated procedures and expensive equipment, reducing the prospect of cost-effectiveness. The method of introducing nanoparticles, which can be cost effective, has shown promises of improving light trapping in the heterojunctions.

Use of the noble nanoparticles for light trapping originates from an enhanced scattering efficiency associated with the localized surface plasma resonance of the particles (Jang et al. 2016). Cao et al. (2014) studied the effect of Ag nanoparticles of diameter 20–50 nm embedded in a poly(3-hexylthiophene) (P3HT) thin film both numerically and experimentally. Their results show that the interference between the incident field and the scattered field of the particles leads to a field enhancement and thus improves the efficiency of organic thin-film solar cell devices. Their results are consistent with findings with the use of other metal nanoparticles reported by researchers (Kalfagiannis et al. 2012; Liu et al. 2014; Shahin et al. 2012). Besides, dielectric particles (e.g., SiO_2) have been discussed in literature for their potential applications in biomedical field (Cheng et al. 2017a, b, c, d; Zeng et al. 2017). Incorporation of SiO_2 nanoparticles of diameter up to 100 nm into the heterojunctions was attempted by for light trapping in organic solar cells (Gollu et al. 2015; Shao et al. 2017).

In this study, we consider a nanoparticle-based approach for the light-trapping enhancement in organic bulk heterojunctions, by which dielectric nanoparticles (SiO_2) are placed atop and noble metal nanoparticles (Ag) inside the active layer to take advantage of best possible electromagnetic scattering effects by each of these types of nanoparticles. Different from studies presented above, the present work intends to explore the synergic coupling of plasmonic scattering effect of Ag nanoparticles with the whispering gallery modes of SiO_2 nanoparticles. Our results show that such an approach, based on a synergic coupling of two particle scattering mechanisms, can produce an impressive improvement of the short-circuit current density in the heterojunctions by up to 42.47%, better than those reported in the above reported studies.

Experimental section

Preparation of particles

The Ag nanoparticles were synthesized following the method of the reduction of silver nitrate by sodium citrate (Li et al. 2013; Turkevich et al. 1951). Typically, 50 μL of the aqueous solution of ascorbic acid (AA) with the concentration ranging 0.10 mM was added into 47.5 mL of boiling water, followed by boiling for an additional 1 min. Also, 1 mL of the aqueous solution of sodium citrate (1 wt.%), 0.25 mL of 1 wt.% aqueous solution of silver nitrate ($AgNO_3$), and 0.1 mL of 0.06 μM aqueous solution of potassium iodide (KI) were consecutively added to 1.25 mL of water under stirring at room temperature. After 5 min of incubation at room temperature, the mixture solution was injected into the boiling aqueous solutions of AA (just after 1 min boiling after AA addition to boiling water). Then, the reaction solution was further boiled for 1 h under stirring to obtain uniform quasi-spherical Ag particles with a diameter of ~ 20 nm. The SiO_2 colloidal is prepared by the Stöber method and the diameter of the particles was regulated by the ratio of tetraethyl orthosilicate (TEOS) and ammonia (Stöber et al. 1968). In this work, 8 mL ammonia was added to 25 mL ethanol and stirring kept for 30 min to make them uniformly mixed. Three milliliters TEOS was then quickly added to the mixture, and the solution was stirred for 8 h to obtain SiO_2 colloids with a diameter of ~ 500 nm.

Preparation of organic solar cells

The basic organic solar cell heterojunction was firstly prepared on a glass slide (or substrate) with a patterned 80 nm indium tin oxide (ITO) layer as anode. The active layer had a poly (3-hexylthiophene):[6,6]-phenyl-C61-butyric acid methyl ester (P3HT:PCBM) weight ratio of a 1:0.6 with a concentration of 25 mg/mL dispersed in the chlorobenzene. Then, the transport layer 3,4-ethylene dioxythiophene:polystyrene sulfonate (PEDOT:PSS) and the P3HT:PCBM layer were successively spin-coated on the glass substrate with the thickness of ~ 40 and ~ 80 nm, respectively. Finally, a 100-nm Al layer is sputtered atop as

cathode to finish the ITO/PEDOT:PSS/P3HT:PCBM/Al structured organic solar cell. Also, the Ag-incorporated solar cell was fabricated by spin-coating the Ag-doped PEDOT or P3HT colloids as the functional layer of the organic solar cell. In detail, the prepared Ag colloids were centrifuged once and re-dispersed in ultrapure H_2O, which was followed by drying in a vacuum oven at 50 °C. Afterwards, the Ag particles were added to PEDOT and P3HT with a concentration of 2.5 wt.%. Then, either the PEDOT or the P3HT colloids were stirred for 12 h at room temperature to make Ag particles well dispersed.

A monolayer of SiO_2 particles was fabricated on the glass slide by the following procedure. First, the prepared colloids were purified by repeated centrifugations (5 cycles) and then re-dispersed in butyl alcohol with a concentration of 10% in weight. Then, a closely arranged SiO_2 particle monolayer forms on the water in a petri dish with a size of 6 cm by dropping 10 μL of the colloid because of the immiscibility of the *n*-butyl alcohol and water (Moon et al. 2011). Finally, a closely arranged particle array was coated on the solar cell device by directly transferring the particle monolayer.

Characterization

The SiO_2 nanoparticles were examined by the scanning electron microscopy (SEM, model: Hitachi 8100) and dynamic light scattering (DLS, model: Beckman Coulter, DelsaNano C). The Ag nanoparticles were characterized by the transmission electron microscopy (TEM, model: JEOL-2100F). The light absorption efficiency of the solar cells was measured by the UV-VIS-NIR spectrophotometer (model: Shimadzu UV3600). Specifically, the light transmission and reflection were measured at a sampling interval of 0.5 nm in the wavelength range of 350 to 800 nm. The absorption efficiency then was calculated from the measured transmission and reflection data. The solar cell performance measuring system includes a sample stage, a solar simulator, a digital source meter, and a processing computer. The organic cell was placed on the sample stage and then illuminated by the solar simulator (AM1.5G). The measured I-V data was acquired by a digital source meter (model: Keithley 2400), which was used to calculate the short-circuit current J_{sc}, the open-circuit voltage V_{oc}, the power conversion efficiency (PCE), and the fill factor (FF) of the solar cell.

Results and discussion

Effect of SiO_2 nanoparticles

Prior to discussing the synergic scattering mechanism, the effect of SiO_2 nanoparticles as light scatters is considered first for the configuration shown in the inset of Fig. 1a, where a monolayer of SiO_2 nanoparticles is placed atop the organic heterojunction (the glass side). It appears that such a particle-organic-heterojunction configuration has not yet been studied in literature, in particular, in terms of the nanoparticle effects on the heterojunction. To further understand the role of the nanoparticles in the system, the finite-difference time-domain (FDTD) simulation was performed by the commercial software of Lumerical. For the simulation, periodic boundary conditions were applied in the x and y directions to simplify the model for the hexagonally arranged particle array. The x-polarized plane wave was incident normally on the structure along the negative z direction. Here, the glass substrate of 120 nm thick is assumed to have a negligible extinction coefficient of glass over the wavelength range from 350 to 800 nm. The FDTD-calculated absorption spectral curves of SiO_2 particles with varying particle sizes are given in Fig. 1a. Apparently, the small-sized SiO_2 particles can improve the efficiency of light absorption in the wavelength range from 350 to ~ 600 nm. This may be attributed to the fact that the monolayer with closely arranged SiO_2 particles atop the cell acts collectively as an anti-reflector by the forward scattering, allowing more incident energy to be introduced into the photoactive layer.

For a larger-sized SiO_2 particle (e.g., $D = 500$ nm), an abrupt absorption peak occurs at the wavelength of ~ 640 nm, in addition to the improved absorption from 350 to 600 nm (see Fig. 1a). Figure 1b shows the distribution of the electric field over the cross section of the SiO_2 sphere along the direction of the polarized field at $\lambda = 640$ nm, and the field is characterized by whispering gallery mode (WGM) excitation (Grandidier et al. 2011, 2012; Yao et al. 2012). Thus, the SiO_2 particles appear to act as a light energy storage device, trapping the incident light at this resonance frequency, and then transfer the trapped energy to the glass substrate and function layers below through leaky mode radiation. The leaky mode radiation causes photons to enter into the photoactive layer, leading to an improvement of the light absorption efficiency.

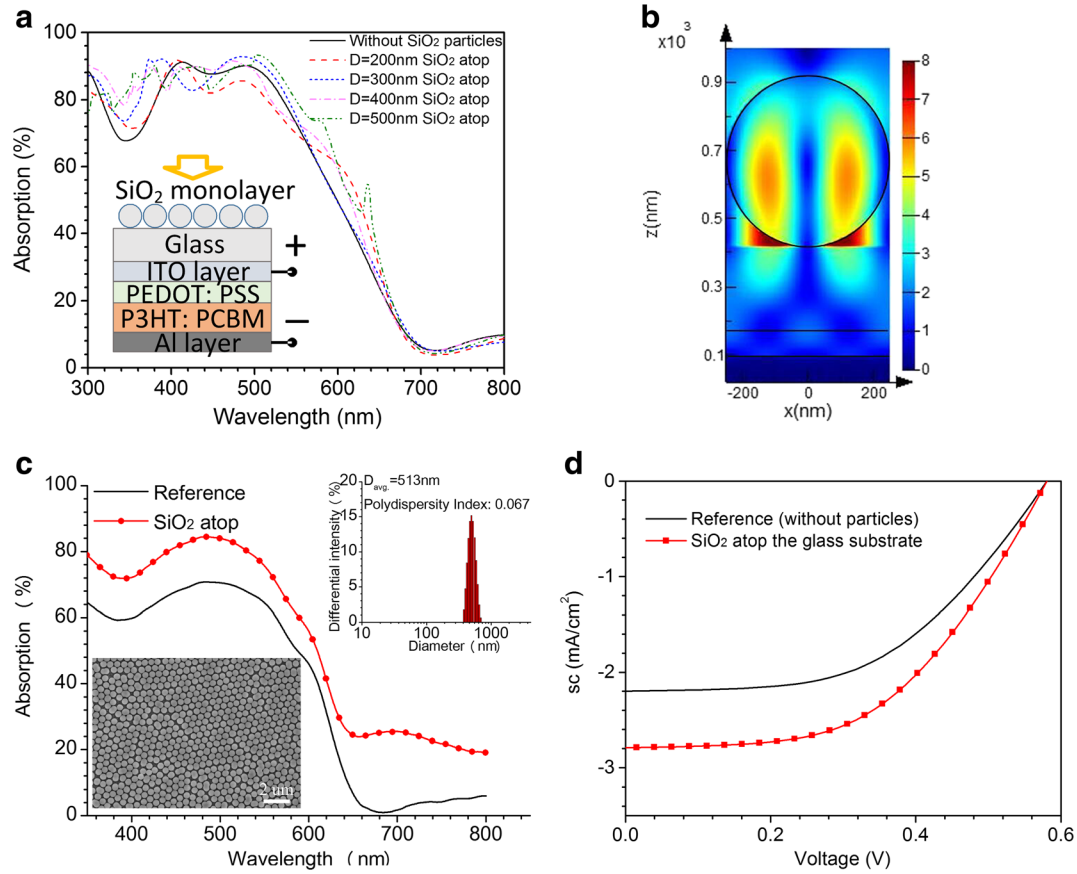

Fig. 1 Absorption enhancement by the presence of SiO_2 nanoparticles: **a** the simulated absorption curves of the P3HT film with varied size SiO_2 particles atop; **b** the electric field distribution of the cross-section along the incident direction at the wavelength of 640 nm; **c** the experimental absorption of the device with/without $D = 513$ nm SiO_2 atop; and **d** the *J-V* characteristics of the device with/without SiO_2. The inset in **a** shows the schematic diagram of SiO_2 particle-coated functional layers, and the insets in **c** show the size distribution of SiO_2 colloids by intensity the SEM image of a monolayer of SiO_2 particles

To confirm the calculations performed above, experiments were conducted. The inset of Fig. 1c shows that SiO_2 nanoparticles have an average diameter of 513 nm and a polydispersity index of 0.067. Also, the patterned monolayer of SiO_2 array was presented. The photo spectrometer measurement of light absorption for this configuration is shown in Fig. 1c. Clearly, a mild and flat broadband enhancement is found over the wavelength region from 650 to 800 nm in the measured absorption efficiency, consistent with the general trend predicted by the FDTD predictions. The measured absorption curve being broad and flattened is attributed to the fact that the SiO_2 particles in the experiment are not perfectly identical in diameter. It is noted that the broadband absorption enhancement is often more desirable for light-trapping applications in energy harvesting.

The measured enhancement of short-circuit current in the heterojunctions with and without the SiO_2 layer is compared in Fig. 1d and other performance parameters measured for the two cases (e.g., open-circuit voltage (V_{oc}), short-circuit current (J_{sc}), fill factor (FF), and power conversion efficiency (PCE)) are given in Table 1. It is noticed from Table 1 that two cases have the same open-circuit current ($V_{oc} = 0.58$ V), because the recombination rate is unchanged by the presence of the SiO_2 particles. For the case without SiO_2, a J_{sc} of 2.19 mA/cm^2, a FF of 58%, and a resulting efficiency of 0.65% are observed. With the SiO_2 nanoparticles placed atop, the J_{sc} increased to 2.80 mA/cm^2 or an improvement of 27.85%, and the PCE increased to 0.81%. This improved performance with the presence of SiO_2 nanoparticles is clearly a direct result of more light being directed into the photoactive layer through

Table 1 Device performance of solar cell with/without SiO_2 atop

	J_{sc} (mA cm^{-2})	V_{oc} (V)	FF (%)	PCE (%)
Without SiO_2	2.19	0.58	50	0.65
With SiO_2	2.80	0.58	51	0.81

whispering gallery mode excitation and leak mode radiation, which leads to the generation of more charge carriers for current transport.

Effect of Ag nanoparticles

The effect of Ag nanoparticles for light trapping is now considered. Ag nanoparticles with small size ($D = \sim$ 20 nm) were prepared (see inset of Fig. 2a) and introduced into the thin anode buffer layer (PEDOT:PSS) or photoactive layer (P3HT:PCBM). These Ag nanoparticles were dispersed in the function layer, P3HT:PCBM layer, or PEDOT:PSS layer, with a concentration of 2.5 wt.%. The absorption efficiency of these two cases was measured by spectrometer and the results for the two cases with and without Ag nanoparticles are given in Fig. 2a. Clearly, the particles dispersed in the P3HT layer or in the PEDOT layer led to much improved light absorption, with the former performing better than the latter. Such an improvement is known to come from the local surface plasma resonance scattering of the Ag particles, which increases the effective optical length, thereby trapping more incident light in the photoactive layer.

It is known that for an organic heterojunction, a higher light-trapping rate with embedded Ag nanoparticles does not yield an enhanced electric field in the P3HT layer. In fact, for the present study, the measured results show that the field is the weakest among the three cases under study, as is evident in the measured *J-V* curves in Fig. 2b and measured data of J_{sc} and PCE in Table 2. Though the embedded Ag particles in the P3HT layer produce more charge carriers due to a strong localized surface plasma resonance, these charge carriers (hole and electron) tend to move along the local field lines of the Ag particle network in the P3HT layer and, consequently, are more likely to recombine with each other (Shen et al. 2009; Xue et al. 2011). Thus, a net gain of charge carriers in the system is not consistent with the light absorption rate. As a result, the power conversion efficiency actually decreased. On the other hand, the Ag particles dispersed in the PEDOT layer scatter light via the surface plasma resonance. The scattering leads to an enhancement of the electric field in the P3HT layer and yet is not strong enough to cause a recombination of the charge carriers. Consequently, a dispersion of Ag particles in the transport layer yields a better *J-V* performance.

Effect of synergic scattering of SiO2 and Ag nanoparticles

As discussed above, the SiO_2 and Ag nanoparticles each produce light-trapping enhancement but through different scattering mechanisms. It is thus logic to consider if

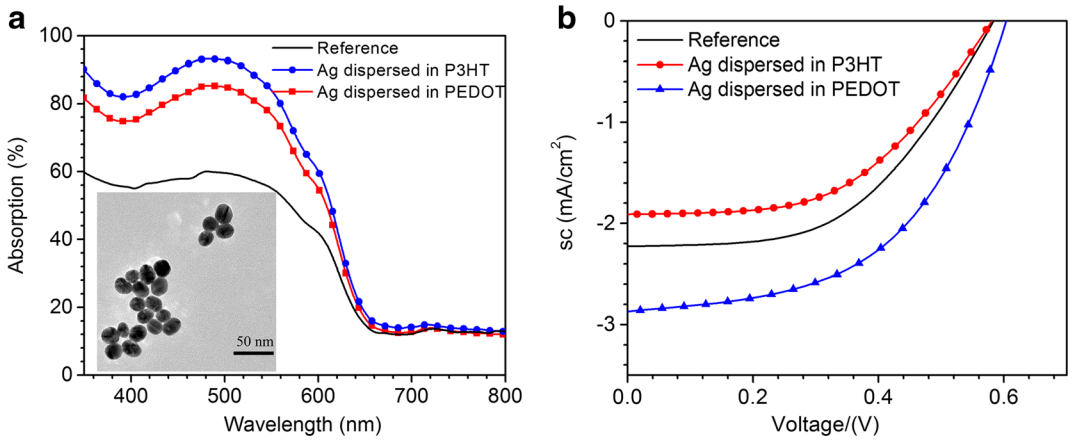

Fig. 2 Effect of Ag nanoparticles on light trapping in an organic solar cell: the experimental absorption (**a**) and the *J-V* (**b**) curves of the device with Ag particles dispersed in active layer and transport layer. The inset in **a** shows the TEM image of prepared $D = 20$ nm of Ag particles

Table 2 Device performance of the solar cell with Ag particle dispersed in P3HT or PEDOT layer

	J_{sc} (mA cm^{-2})	V_{oc} (V)	FF (%)	PCE (%)
Without Ag	2.19	0.58	50	0.65
Ag in P3HT	1.91	0.58	50	0.57
Ag in PEDOT	2.85	0.60	52	0.87

Table 3 Device performance of the solar cell with Ag, SiO_2, and Ag and SiO_2

	J_{sc} (mA cm^{-2})	V_{oc} (V)	FF (%)	PCE (%)
Reference	2.19	0.58	50	0.65
SiO_2 atop	2.80	0.58	51	0.81
Ag in PEDOT	2.85	0.60	52	0.87
Ag and SiO_2	3.12	0.61	52	1

these two different scattering mechanisms can be managed to produce a synergic coupling effect. To explore this effect, a structured device was prepared, where the 513-nm SiO_2 particles were arranged atop and the 20-nm Ag particles dispersed in the PEDOT layer. The structure was fabricated by first dispersing the Ag particles in the PEDOT layer and then by arranging a SiO_2 layer on the glass. The *J-V* measurements were conducted on the structured device. The FDTD simulation was also performed, for which the Ag particles are assumed to be periodically arranged with an interparticle distance of $d = 62.5$ nm (estimated) inside the PEDOT layer. The results are given in Fig. 3. Comparison of the field distributions at the resonance wavelength of $\lambda = \sim$ 640 nm in Fig. 3a, b reveals a strong collaborative coupling of light scattering into the P3HT layer by the SiO_2 nanoparticles via the excitation of WGM in the particles and leak mode radiation and by the Ag nanoparticles via excitation of the localized surface plasma. In the case where the SiO_2 particles were absent (see Fig. 3b), the localized surface plasma resonance fields of the Ag particles were rather confined around the particles and the symmetrically enhanced regions around the particle were parallel with polarized direction of the incident light. With the presence of the SiO_2 nanoparticles atop, the light scattered into the heterojunction by the leak mode radiation further interacts with the Ag nanoparticles embedded in the device to further excite the localized surface plasma, thereby producing a stronger field than by either of these particles alone (see Figs. 1b and 3b). And the enhanced regions around the Ag particles were guided by the leaky mode of the WGM of the SiO2 atop and most of enhanced energy was scattered into the photoactive layer to prolong the effect optical path. In other words, a substantial increase of the effective optical length of the incident light and hence a much better light-trapping efficiency in the heterojunction are achieved by this synergic coupling of WGM/leak mode radiation associated with the SiO_2 atop and the localized surface plasma resonance scattering by the Ag particles inside.

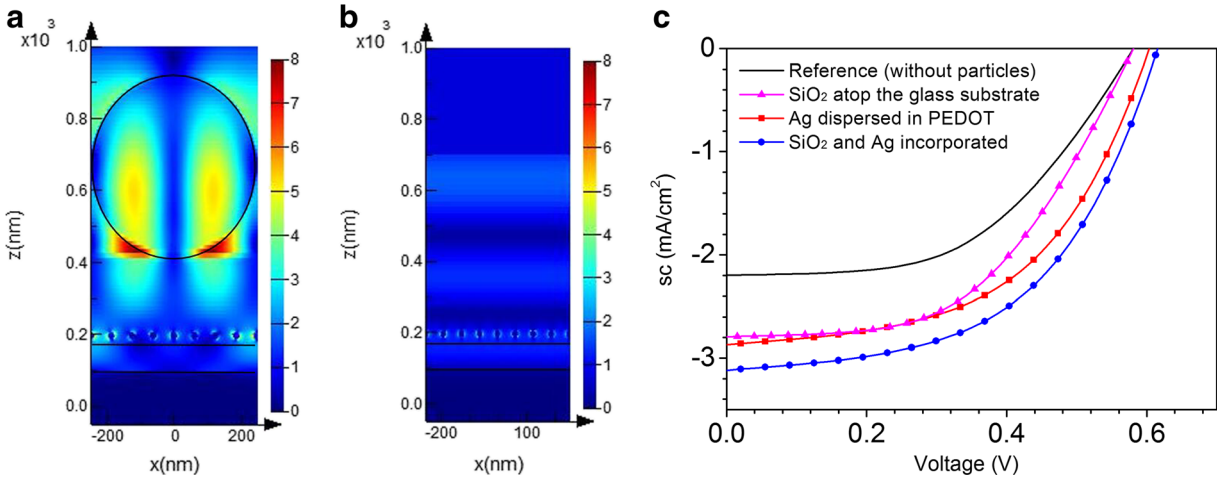

Fig. 3 Synergetic scattering of SiO_2 and Ag nanoparticles for light trapping: the electric field distribution of the cross section along the incident direction at the wavelength of 640 nm of the cell **a** with SiO_2 and **b** without SiO_2 and **c** the *J-V* characteristics of the device incorporated with Ag, SiO_2, and both Ag and SiO_2

The measured short-circuit current density J_{sc} of the structured heterojunction is given in Fig. 3c, where the data for other cases are also included for the sake of comparison. The measured *J-V* characteristics and relevant data are listed in Table 3. Examination of these measured data clearly indicates that the heterojunction structure with synergetic scattering of SiO_2 and Ag nanoparticles perform the best among all these cases. Indeed, as is evident from the data in Table 3, the short-circuit current density J_{sc} of the structured heterojunction was measured at 3.12 mA/cm^2, which is an improvement of 42.47% over the case with neither particle present. The open-circuit voltage (V_{oc}) also increased from 0.58 to 0.61 V and the power conversion efficiency has increased to 1 from 0.65%.

Conclusions

An experimental study has been presented of the coupled light scattering effect and whispering gallery mode of the SiO_2 particles on the photoactive film, the effect of localized surface plasma resonance scattering of Ag particles, and the synergetic scattering of SiO_2 and Ag nanoparticles for light trapping in organic solar cells. It is found that closely arranged SiO_2 particle monolayer atop the device can effectively guide the incident light into the photoactive layer, thereby enhancing the light absorption efficiency of the device. For SiO_2-enhanced device, the short-circuit current density J_{sc} increased from 2.19 to 2.80 mA/cm^2 or an increase by 27.85%. A compromised effect of local field enhancement and carrier recombination resulting from the Ag particles in the transport layer accounts for the improved *J-V* performance. The solar cell structured with ~20 nm Ag particles dispersed in the transport layer and ~500 nm SiO_2 atop the device exploits the salient feature of synergetic scattering of SiO_2 and Ag nanoparticles to generate stable resonance mode in the active layer, leading to the best power conversion performance of the device, among all cases studied. The J_{sc} of this new structured device is 3.12 mA/cm^2, which is a 42.47% improvement over the cell with no nanoparticles present.

Acknowledgements Partial support of this work by the Shaanxi Department of Science and Technology Development (Grant No. 2013KTCQ01-48) is acknowledged.

Compliance with ethical standards

Conflict of interest The authors declare that they have no conflict of interest.

References

Cao Y, Peng D, Qiao Y, Liu Z, Sun Z (2014) Light absorption enhancement of ~ 100 nm thick poly(3-hexylthiophene) thin-film by embedding silver nanoparticles. Appl Phys Lett 105(15):153902. https://doi.org/10.1063/1.4898600

Cheng W, Liang C, Wang X, Tsai H-i, Liu G, Peng Y, Nie J, Huang L, Mei L, Zeng X (2017a) A drug-self-gated and tumor microenvironment-responsive mesoporous silica vehicle: "four-in-one" versatile nanomedicine for targeted multidrug-resistant cancer therapy. Nano 9:17063–17073

Cheng W, Liang C, Xu L, Liu G, Gao N, Tao W, Luo L, Zuo Y, Wang X, Zhang X (2017b) TPGS-functionalized polydopamine-modified mesoporous silica as drug nanocarriers for enhanced lung cancer chemotherapy against multidrug resistance. Small 13(29):1700623. https://doi.org/10.1002/smll.201700623

Cheng W, Nie J, Gao N, Liu G, Tao W, Xiao X, Jiang L, Liu Z, Zeng X, Mei L (2017c) A multifunctional nanoplatform against multidrug resistant cancer: merging the best of targeted chemo/gene/photothermal therapy. Adv Funct Mater 27(45). https://doi.org/10.1002/adfm.201704135

Cheng W, Nie J, Xu L, Liang C, Peng Y, Liu G, Wang T, Mei L, Huang L, Zeng X (2017d) A pH-sensitive delivery vehicle based on folic acid-conjugated polydopamine-modified mesoporous silica nanoparticles for targeted cancer therapy. ACS Appl Mater Interfaces 9(22):18462–18473. https://doi.org/10.1021/acsami.7b02457

Chou C-H, Chen F-C (2014) Plasmonic nanostructures for light trapping in organic photovoltaic devices. Nano 6:8444–8458

Dang MT, Wantz G, Bejbouji H, Urien M, Dautel OJ, Vignau L, Hirsch L (2011) Polymeric solar cells based on P3HT: PCBM: role of the casting solvent. Sol Energy Mater Sol Cells 95(12):3408–3418. https://doi.org/10.1016/j.solmat.2011.07.039

Gan Q, Bartoli FJ, Kafafi ZH (2013) Plasmoni-enhanced organic photovoltaics: breaking the 10% efficiency barrier. Adv Mater 25(17):2385–2396. https://doi.org/10.1002/adma.201203323

Gollu SR, Sharma R, Srinivas G, Kundu S, Gupta D (2015) Incorporation of SiO_2 dielectric nanoparticles for performance enhancement in P3HT: PCBM inverted organic solar cells. Org Electron 24:43–50. https://doi.org/10.1016/j.orgel.2015.05.017

Grandidier J, Callahan DM, Munday JN, Atwater HA (2011) Light absorption enhancement in thin-film solar cells using whispering gallery modes in dielectric nanospheres. Adv Mater 23(10):1272–1276. https://doi.org/10.1002/adma.201004393

Grandidier J, Deceglie MG, Callahan DM, Atwater HA (2012) Simulations of solar cell absorption enhancement using

resonant modes of a nanosphere array. J Photonics Energy 2(1):024502. https://doi.org/10.1117/1.JPE.2.024502

Jang YH, Jang YJ, Kim S, Quan LN, Chung K, Kim DH (2016) Plasmonic solar cells: from rational design to mechanism overview. Chem Rev 116(24):14982–15034. https://doi.org/10.1021/acs.chemrev.6b00302

Kalfagiannis N, Karagiannidis PG, Pitsalidis C, Panagiotopoulos NT, Gravalidis C, Kassavetis S, Patsalas P, Logothetidis S (2012) Plasmonic silver nanoparticles for improved organic solar cells. Sol Energy Mater Sol Cells 104:165–174. https://doi.org/10.1016/j.solmat.2012.05.018

Krebs FC, Alstrup J, Spanggaard H, Larsen K, Kold E (2004) Production of large-area polymer solar cells by industrial silk screen printing, lifetime considerations and lamination with polyethyleneterephthalate. Sol Energy Mater Sol Cells 83(2-3):293–300. https://doi.org/10.1016/j.solmat.2004.02.031

Lee JK, Ma WL, Brabec CJ, Yuen J, Moon JS, Kim JY, Lee K, Bazan GC, Heeger AJ (2008) Processing additives for improved efficiency from bulk heterojunction solar cells. J Am Chem Soc 130(11):3619–3623. https://doi.org/10.1021/ja710079w

Li G, Yao Y, Yang H, Shrotriya V, Yang G, Yang Y (2007) "Solvent annealing" effect in polymer solar cells based on poly (3-hexylthiophene) and methanofullerenes. Adv Funct Mater 17(10):1636–1644. https://doi.org/10.1002/adfm.200600624

Li G, Zhu R, Yang Y (2012) Polymer solar cells. Nat Photonics 6(3):153–161. https://doi.org/10.1038/nphoton.2012.11

Li H, Xia H, Wang D, Tao X (2013) Simple synthesis of monodisperse, quasi-spherical, citrate-stabilized silver nanocrystals in water. Langmuir 29(16):5074–5079. https://doi.org/10.1021/la400214x

Liu Z, Lee SY, Lee EC (2014) Copper nanoparticle incorporated plasmonic organic bulk-heterojunction solar cells. Appl Phys Lett 105(22):223306. https://doi.org/10.1063/1.4903749

Luo G, Ren X, Zhang S, Wu H, Choy WC, He Z, Cao Y (2016) Recent advances in organic photovoltaics: device structure and optical engineering optimization on the nanoscale. Small 12(12):1547–1571. https://doi.org/10.1002/smll.201502775

Ma W, Yang C, Gong X, Lee K, Heeger AJ (2005) Thermally stable, efficient polymer solar cells with nanoscale control of the interpenetrating network morphology. Adv Funct Mater 15(10):1617–1622. https://doi.org/10.1002/adfm.200500211

Mariani G, Laghumavarapu RB, Bertrand TDV, Shapiro J (2010) Hybrid conjugated polymer solar cells using patterned GaAs nanopillars. Appl Phys Lett 97(1):013107. https://doi.org/10.1063/1.3459961

Moon GD, Lee TI, Kim B, Chae GS, Kim J, Kim SH, Myoung JM, Jeong U (2011) Assembled monolayers of hydrophilic particles on water surfaces. ACS Nano 5(11):8600–8612. https://doi.org/10.1021/nn202733f

Na SI, Kim SS, Kwon SS, Jo J, Kim J, Lee T, Kim DY (2007) Surface relief gratings on poly(3-hexylthiophene) and fullerene blends for efficient organic solar cells. Appl Phys Lett 91(17):173509. https://doi.org/10.1063/1.2802561

Nalwa KS, Park JM, Ho KM, Chaudhary S (2011) On realizing higher efficiency polymer solar cells using a textured substrate platform. Adv Mater 23(1):112–116. https://doi.org/10.1002/adma.201002898

Niggemann M, Glatthaar M, Gombert A, Hinsch A, Wittwer V (2004) Diffraction gratings and buried nano-electrodes—architectures for organic solar cells. Thin Solid Films 451:619–623

Shahin S, Gangopadhyay P, Norwood RA (2012) Ultrathin organic bulk heterojunction solar cells: Plasmon enhanced performance using au nanoparticles. Appl Phys Lett 101:6335

Shao P, Chen X, Guo X, Zhang W, Chang F, Liu Q, Chen Q, Li J, Li Y, He D (2017) Facile embedding of SiO2 nanoparticles in organic solar cells for performance improvement. Org Electron 50:77–81. https://doi.org/10.1016/j.orgel.2017.07.029

Shen H, Bienstman P, Maes B (2009) Plasmonic absorption enhancement in organic solar cells with thin active layers. J Appl Phys 106(7):073109. https://doi.org/10.1063/1.3243163

Stöber W, Fink A, Bohn E (1968) Controlled growth of monodisperse silica spheres in the micron size range. J Colloid Interface Sci 26(1):62–69. https://doi.org/10.1016/0021-9797(68)90272-5

Turkevich J, Stevenson PC, Hillier J (1951) A study of the nucleation and growth processes in the synthesis of colloidal gold. Discuss Faraday Soc 11:55–75. https://doi.org/10.1039/df9511100055

Xue M et al (2011) Title: charge-carrier dynamics in hybrid plasmonic organic solar cells with Ag nanoparticles. Appl Phys Lett 28:253302

Yang F, Forrest SR (2008) Photocurrent generation in nanostructured organic solar cells. ACS Nano 2(5):1022–1032. https://doi.org/10.1021/nn700447t

Yao Y, Yao J, Narasimhan VK, Ruan Z, Xie C, Fan S, Cui Y (2012) Broadband light management using low-Q whispering gallery modes in spherical nanoshells. Nat Commun 3:664. https://doi.org/10.1038/ncomms1664

Yu G, Gao J, Hummelen JC, Wudl F, Heeger AJ (1995) Polymer photovoltaic cells - enhanced efficiencies via a network of internal donor-acceptor heterojunctions : enhanced efficiencies via a network of internal donor-acceptor heterojunctions. Science 270(5243):1789–1791. https://doi.org/10.1126/science.270.5243.1789

Zeng X, Liu G, Tao W, Ma Y, Zhang X, He F, Pan J, Mei L, Pan G (2017) A drug-self-gated mesoporous antitumor nanoplatform based on pH-sensitive dynamic covalent bond. Adv Funct Mater 27(11):1605985. https://doi.org/10.1002/adfm.201605985